

THE PWN TORUS OF PSR J0538 + 2817 AND THE ORIGIN OF PULSAR VELOCITIES

ROGER W. ROMANI & C.-Y. NG
 Department of Physics, Stanford University, Stanford, CA 94305
 rwr@astro.stanford.edu, ncy@astro.stanford.edu
ApJ submitted

ABSTRACT

We find evidence for a faint wind nebula surrounding PSR J0538 + 2817 in *CXO-ACIS* imaging. This object is particularly interesting, as the pulsar spindown age is largest for any such X-ray PWN. If interpreted as an equatorial torus, the PWN supports the claimed association with the S147 supernova remnant and implies good alignment between the pulsar spin and space velocity. Comparison of the SNR age, X-ray cooling age and characteristic age suggests a birth spin period of $\gtrsim 130$ ms. In turn, if we accept as causal the alignment of the linear and angular momenta, this places strong constraints on the origin of the ‘kick’ at the neutron star birth.

Subject headings: stars: neutron – pulsars – stars: rotation

1. INTRODUCTION

Hubble Space Telescope and, especially, *Chandra X-ray Observatory (CXO)* imaging have discovered toroidal structure in the synchrotron pulsar wind nebulae (PWN) of relativistic particles and magnetic fields around young neutron stars (e.g. Weisskopf *et al.* 2000, Pavlov *et al.* 2001, Gotthelf 2001). Of these, the Crab and Vela pulsar tori are the most striking, with clear symmetry (pulsar spin) axes. Moreover, for these two objects *HST* proper motion studies show alignment between the position angles of the projected $\vec{\Omega}$ and \vec{v} . The chance probability of two such alignments is modest, but if taken as causal this gives strong constraints on nature of the ‘kick’ at pulsar birth which typically produces a large space velocity (Spruit & Phinney 1998, Lai *et al.* 2001). Even a few further examples could improve the statistical significance of the $\vec{\Omega}$ - \vec{v} correlation and further constrain the kick physics (§4). The challenge is to identify sources for which both PWN tori and 2-D proper motions are measurable; after the Crab and Vela, many bright young PSR/PWN sources are quite distant and direct proper motion measurement is challenging. We report here on *CXO* imaging of one particularly interesting example.

PSR J0538+2817, discovered by Anderson *et al.* (1996) is a 143ms pulsar with characteristic age $\tau_c = 6 \times 10^5$ y. Located within the old $\sim 10^5$ y SNR S147 (G180.0–1.7) with a DM-estimated distance of 1.2kpc (Cordes & Lazio 2002) comparable to that of the SNR, it is believed to be a likely association despite the age discrepancy. Previously reported X-ray observations are limited to *ROSAT* all sky survey (Sun *et al.* 1996) and *HRI* imaging. Inspection of the archival *HRI* data showed a source slightly extended beyond the nominal PSF, although aspect errors may have contributed. We have obtained *ACIS-S* imaging to resolve this possible PWN.

2. *CXO* OBSERVATIONS

We observed PSR J0538 + 2817 with the *CXO ACIS* on February 7-8, 2002, with the pulsar near the S3 chip aim-point, obtaining 19.5ks of TE exposure. All 6 *ACIS* chips were active and several field sources were detected off axis. None showed markedly unusual behavior; we there-

fore concentrate on the S3 pulsar data. Calibration, processing and spectral fitting were performed with CIAO 2.3, including the latest calibrations and CTE corrections.

2.1. Spatial Decomposition

The pulsar core produces 0.13 cnts/s and, with the standard 3.2s *ACIS* frame, suffers 20% pileup. In Figure 1 we compare the 0.5-5 keV source radial profile with that of the HRMA+*ACIS* model PSF (generated for the observed source count spectrum and corrected for pileup). The point source normalization has been obtained from a PSF fit to the central 3". The core is resolved, with $\sim 10\%$ of the counts in extended emission. If the PSF is convolved with a $\sigma = 1''$ Gaussian, the counts are well matched out to 5", but a 5σ excess remains above background from 5–8". We thus believe that the extended emission cannot be attributed to aspect errors or poor PSF modeling.

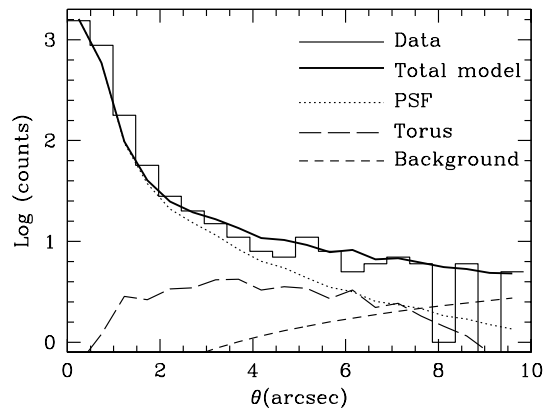


FIG. 1.— Source and model radial count distributions.

This emission does not follow the symmetric PSF wings (Figure 2). We start by fitting elliptical isophotes, with semi-major axes from 1-10", using the STSDAS routine *ellipse*. For small 1 – 2.5" semi-major axes, we find an ellipticity of $\sim 0.1 - 0.2$ at position angle $\sim 130^\circ$ (measured N-E). From 4 – 9" the PA changes to a weighted average value of $61.0 \pm 5.5^\circ$ with an ellipticity of 0.25-0.35. In Figure 2, the core has a tail to the SE defining the inner ellipse, while the scattered photons along the NE-SW axis

represent the larger ellipse. Some trailing along the read-out direction is visible in the detector coordinate image (at PA= 91°), but cannot be seen in Figure 2. The measured trail flux contributes less than 1 count in the 10'' region of our extended emission, and does not lie along the axis of extension.

In analogy to other pulsar/PWN systems we can expect a toroidal wind shock surrounding the pulsar, possibly with a polar jet. The 4 – 9'' ellipse has a scale comparable to the expected wind shock radius for a confinement pressure appropriate to the interior of S147 (see §3). We therefore adopt this physical model, computing the expected photons from the point source PSF wings and fitting the excess photons outside of 3'' to an inclined torus. A uniform background for the residual counts is also allowed. The torus model is characterized by a radius r_T , a Gaussian blur torus thickness δ , the position angle Ψ of the torus axis and its inclination ζ from the observer line of sight. We assume that the post-shock flow remains relativistic, so that the emission is Doppler boosted in the forward direction. For a rest power law emission spectrum $dN'_\gamma/dE_\gamma \propto E_\gamma^{-\alpha}$, we expect an observed emissivity

$$dN_\gamma/dE_\gamma \propto (1 - \mathbf{n} \cdot \beta)^{-(1+\alpha)} E_\gamma^{-\alpha}$$

where α is the photon spectral index, $\beta = \mathbf{v}/c$ is the bulk velocity of the post shock flow and \mathbf{n} is the unit normal toward the observer (e.g. Pelling *et al.* 1987). For typical PWNe, $\alpha \approx 1.5$ and the emission brightens on the side facing the observer.

Of the 2875 counts in the central 32'' × 32'' region, the best-fit point source provides 2430, the uniform background contributes 80 counts and the ‘torus’ provides 50 counts. The remaining counts represent unresolved fine structure in the nebula core. The best-fit torus radius is $r_T = 7.2 \pm 0.7''$, the ‘blur’ scale is $\delta = 1.9 \pm 0.5''$. The torus β is 0.53 ± 0.04 , similar to values fit for other PWN. The torus symmetry axis is located at position angle $\Psi = 154.0 \pm 5.5^\circ$ (measured N through E) and $\zeta = 100 \pm 6^\circ$ (into the plane of the sky), where the confidence regions have been scaled to that of Ψ .

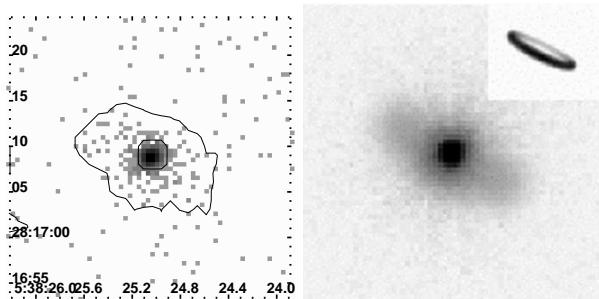


FIG. 2.— *Left*: ACIS 0.5-5 keV image with smoothed low level contours. *Right*: Best-fit Point Source + torus model. *Inset*: Best-fit torus model at half scale, with δ reduced to 0.5'' to show geometry.

In Figure 2 we show the photon data and the predicted image for the best-fit point source + torus model. The position angle Ψ is robust to cuts in the fit data set and forced variations in r_T and δ and agrees well with the value determined from ellipse isophote fits; we adopt this value as determining the symmetry axis. ζ , primarily set by the ellipse axis ratio, is also surprisingly well determined. The brightening of the diffuse emission SE of the core indicates

the near side of the torus, enhanced by Doppler beaming (inset). However, the core asymmetry also suggests a ‘polar jet’. Certainly deeper exposures would be quite valuable in confirming the reality of these faint structures and measuring their precise parameters.

2.2. Spectral Analysis

We extract the point source from a 2'' aperture, correcting for pileup and measuring a nearby background from the S3 chip. For the torus we take a $\sim 10'' \times 18''$ ellipse with a 4'' radius exclusion core. The PSF wings of the central source contribute significant counts in this aperture, so we include a scaled version of the best-fit point source spectrum as a fixed background and fit the excess to characterize the torus emission.

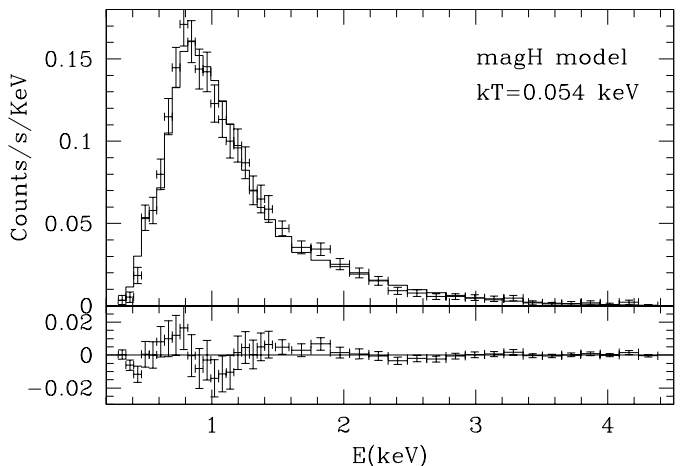


FIG. 3.— Point source spectrum with a pileup-corrected magnetic H model atmosphere spectrum and residuals.

The point source spectrum is adequately modeled by an absorbed blackbody, although systematic residuals persist at low energies. Table 1 gives the fit parameters with 95% errors, the unabsorbed bolometric flux and the effective radius of a spherical emitter at $d = 1.2\text{kpc}$. The second fit is from the magnetic H atmosphere models of Pavlov, *et al.* (1995), which produce slightly better χ^2 and a larger effective radius. We note that all of these fits are somewhat suspect, since the spatial decomposition suggests $\sim 10\%$ diffuse emission even for the core. Composite (BB+BB or BB+PL) models of course improve the fit statistics, but are not demanded by the present data. These fits give N_H somewhat larger than the $\sim 1.2 \times 10^{21}\text{cm}^{-2}$ inferred from the pulsar DM with a canonical $n_e/n_H \approx 10$.

A comparison of the energies of the 51 torus photons outside of 4'' with the 240 photons from 1 – 2'' (which avoid pile-up in the point source core) gives a KS statistic probability of 0.06 that they are drawn from the same distribution. The torus region photons are thus significantly harder than the point source (despite the 30% contamination by the PSF wings); this further supports the independent nature of this component. We assume a PL model for this torus emission. Fixing N_H as above and assuming a typical PWN $\Gamma = 1.5$, we find an unabsorbed flux $f_X(0.5 - 5\text{ keV}) \approx 1.6 \pm 0.4 \times 10^{-14}\text{erg/cm}^2/\text{s}$ for the full torus. This spindown efficiency $\eta \approx 6 \times 10^{-5} d_{1.2}^2$ is about $10\times$ lower than that of most $\tau \sim 10^4\text{y}$ pulsars.

3. THE SNR ASSOCIATION & KICK-SPIN CORRELATION

S147 is a late blast wave phase SNR, quite circular in both radio (Fürst & Reich 1986) and H α (van den Bergh 1978) images, with a $\sim 166'$ diameter. The estimated 0.8-1.6 kpc distance agrees very well with the pulsar's 1.2 kpc DM-derived distance. Sofue, Fürst & Hirth (1980) find the geometrical center at 05:40, +27:44 ($\pm 2.5'$) (J2000). At the nominal distance the $\gamma = 5/3$ Sedov solution gives a blast wave age of $t = 1.4 \times 10^5 d_{1.2}^{5/2} (n/E_{51})^{1/2}$ y and an expansion velocity $v_{\text{exp}} = 82 d_{1.2}^{-3/2} (E_{51}/n)^{1/2}$ km/s for a local ISM density $n \text{ cm}^{-3}$ and an explosion energy $10^{51} E_{51}$ erg. The optical expansion velocity ≈ 80 km/s (Kirshner & Arnold 1979) agrees well, supporting the distance estimate.

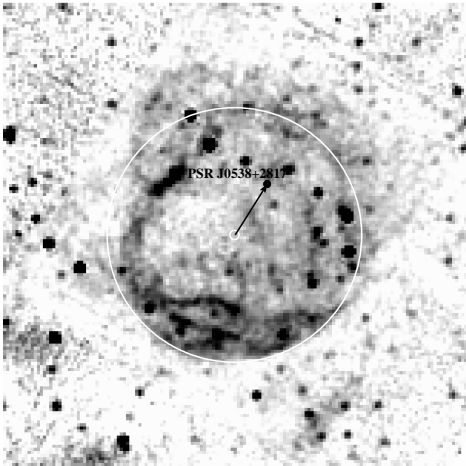


FIG. 4.— 11cm image of S147 (after Fürst & Reich 1986), with PSR J0538 + 2817 's proper motion vector (3° field, N up/E left).

If we assume magnetic dipole spindown ($n = 3$) with a constant field $10^{12} B_{12}$ G, the spindown luminosity at characteristic age $10^5 \tau_5$ y is

$$\dot{E} = 1.0 \times 10^{36} (B_{12} \tau_5)^{-2} \text{ erg/s,}$$

leading to a scale for the wind termination

$$r_T \approx (\dot{E}/4\pi c P_{\text{ext}})^{1/2}.$$

This termination will be azimuthally symmetric (e.g. toroidal) whenever the external static pressure $P_{\text{ext}} \geq P_{\text{ram}} = 6 \times 10^{-10} n v_7^2 \text{ g/cm/s}^2$, i.e. subsonic pulsar motion at a speed $100 v_7$ km/s. In the general ISM, P_{ext} is typically a few $\times 10^{-13} \text{ g/cm/s}^2$; all but the slowest young pulsars should display non-toroidal bow shocks. However, in the interior of a Sedov-phase SNR we have $P_{\text{ext}} \approx 6 \times 10^{-11} (n_0^3 E_{51}^2 / t_5^6)^{1/5} \text{ g/cm/s}^2$ where the ambient ISM density is n_0 and we have distinguished between the true (=SNR) pulsar age t and the characteristic age τ_c . Since the density in the hot interior is quite low, eg. $\text{Log}(n_i) = \text{Log}[n_0(2r/r_{\text{Sed}} - 2)]$ (Mansfield & Salpeter 1974), we expect pulsars in the interior of SNR to be in the toroidal shock phase for $t_5 \lesssim 3$. The difficulty is that at typical speeds of $v_7 \approx 5$, a pulsar outruns the blast wave by $t_5 \approx 0.3 (E_{51}/n_0)^{1/3} (v_7/5)^{-5/3}$. In fact, as soon as it passes the contact discontinuity, the large density and ram pressure jump ensure a bow shock morphology. PSR 1951+32 in CTB 80 is likely in this phase (Shull *et al.* 1988).

According to these estimates, a torus for PSR J0538 + 2817 is not unexpected. At $t_5 \gtrsim 1$ we would normally find

it in the ambient ISM, but its low $v_7 \approx 1.5/t_5$ keeps it in its host SNR. With a low $B_{12} = 0.74$, the pulsar husbands its spin-down luminosity giving a torus of angular size

$$\theta_{\text{tor}} = r_T/d \approx 14'' (B_{12} d_{\text{kpc}} \tau_5 n_0^{0.3} E_{51}^{0.2} t_5^{-0.6})^{-1}$$

or about $3'' t_5^{0.6} n_0^{-0.3} d_{1.2}^{-1}$ for PSR J0538 + 2817, among the largest angular sizes expected for known pulsars (after Crab and Vela). Since the observed inner edge of the torus is at $\sim 5''$, these estimates agree if $t_5 \sim 2$ or $n_0 \sim 0.2$.

Given the large offset of PSR J0538+2817 from the remnant center, a good test of the $\vec{\Omega}$ - \vec{v} correlation can be made. The offset vector implies a proper motion $(23.6 \pm 1.5)/t_5$ mas/y at position angle $-32.3 \pm 3.6^\circ$. The pulsar transverse velocity is $134 d_{1.2}/t_5$ km/s. Together with the torus geometry estimates of §2.2, this offset gives a kick-spin position angle difference of $\theta_{\Omega-v} = 6.3 \pm 6.6^\circ$. If \vec{v} is along the torus axis, the 3D velocity is $137 d_{1.2}/t_5$ km/s, rather low for an isolated pulsar.

The Crab pulsar optical proper motion (Caraveo & Mignani 1999) and inner nebula axis vectors give $\theta_{\Omega-v} = 10 \pm 10^\circ$. For Vela, the symmetry axis of the X-ray torus in Pavlov, *et al.* (2001) is aligned within $2 \pm 3^\circ$ (Bailes *et al.* 1989) or $10 \pm 3^\circ$ (De Luca, Mignani & Caraveo 2000) using the radio or optical \vec{v} , respectively. The joint probability of obtaining these (2-D) projections by chance is $\sim 0.3 - 1\%$, making the association intriguing, but not definitive. If one adopt PSR J0538 + 2817 as a third alignment, the chance probability drops to $\sim 2 \times 10^{-4}$.

4. DISCUSSION: AGE AND KICK CONSTRAINTS

One of the key discriminants of the origin of this correlation is the initial pulsar spin period P_0 (Lai, Chernoff & Cordes 2001). For a constant braking index n one finds

$$t = 2\tau_c [1 - (P_0/P)^{(n-1)}] / (n-1).$$

Since our PWN position angle supports the connection with S147, we must reconcile the $\tau_c = 10^{5.8}$ y ($n = 3$) characteristic age with the maximum plausible age $\sim 10^5$ y of the SNR. One possibility is very rapid B decay, giving an effective $n \gtrsim 10$. More likely, as for several other PSR-SNR associations there is a large initial spin period. The observed thermal luminosity supports the young age and large P_0 . This $L \approx 2 \times 10^{33} d_{1.2}^2 \text{ erg/s}$, interpreted as full surface cooling agrees well with the flux in standard cooling scenarios near 10^5 y. At $P_0 \approx 130$ ms ($t_5 \approx 1$) PSR J0538+2817 has one of the slowest initial spins known.

Physical kick-spin connections generally rely on rotational averaging (Spruit & Phinney 1998), so this large P_0 is problematic for many proposed mechanisms. If the kicks are isotropically distributed, the net moment at $\theta \approx 60^\circ$ must be averaged for $\tau_{\text{kick}} \gg 0.38 P_0 / \tan \theta_{\Omega-v}$ to achieve a final spin-kick angle $\theta_{\Omega-v}$. Indeed, since 'Natal' kicks may be applied before the neutron star has reached its final $\sim 10^6$ cm radius, conservation of angular momentum for kicks at $r_6 > 1$ increases the effective initial period by r_6^2 . Thus for PSR J0538 + 2817, we require $\tau_{\text{kick}} \gg 0.5 s (1 - t_5/6)^{1/2} r_6^2$ for the observed $\theta_{\Omega-v}$.

Certainly the E-M rocket (Harrison-Tademaru) effect is hopeless, as it requires $P_0 \lesssim 3$ ms for 100 km/s velocities. Also hydromagnetic models imparting momentum over ~ 0.1 s are inadequate, especially as the momentum

deposition is at the $r_6 \gtrsim 10$ shock break-out. Even mechanisms invoking asymmetric ν emission are severely constrained, but appear just feasible considering the $\sim 3s$ ν diffusion timescale at $r_6 \sim 1 - 2$. However inducing the large required ν asymmetry is challenging. For magnetic-field induced asymmetry, even PSR J0538 + 2817 's modest velocity requires an ordered neutrinosphere field of $\sim 10^{15.5}G$ (Arras & Lai 1999), otherwise unmotivated for this low B pulsar.

As an alternative one may imagine schemes where the spin is driven to the kick axis. One possibility is post-collapse accretion of a remnant disk (Blandford, private comm.). Imagine a disk of $\sim \Delta M$ accreting at a super-Eddington rate onto a $1.5M_{1.5}M_{\odot}$ neutron star with moment of inertia $10^{45}I_{45}gcm^2$. The disk is approximately Keplerian down to some inner radius r_{in} , at which point we assume roughly half of the mass accretes while the remainder is ejected in polar jets with velocity $v_{esc} \approx 2^{1/2}v_{Kep}(r_{in})$ and an asymmetry χ . The large P_0 inferred for PSR J0538 + 2817 is a serious constraint on this scenario. If the disk extends to the star, we might expect jet velocities of $\sim c/4$ as in SS443, but only $\Delta M \approx 2 \times 10^{-3}I_{45}(100ms/P_0) M_{\odot}$ may accrete before one spins up to $P_0 < 0.1s$. With this mass, jet recoil gives a kick $v_K \approx 75\chi/M_{1.5}km/s$ for PSR J0538+2817 's parameters, so that even a large jet asymmetry does not produce the desired momentum.

Perhaps more realistically, standard equilibrium spin-up arguments set $r_{in} = (B_*^2 R_*^6 / \dot{M} \sqrt{2GM_*})^{2/7} \approx 1.8 \times$

$10^8 B_{12}^{4/7} \dot{M}_{-8}^{-2/7} cm$. The Keplerian period at this Alfvén radius is thus comparable to P_0 for $\dot{M}_{-8} \approx 130$, i.e. $\sim 100 \times$ the Eddington accretion rate. If as expected the star is born near a $\sim 1 P_i ms$ break up period, the minimum mass needed to spin down the star to P_0 is $\Delta M \approx 0.04 M_{\odot} I_{45} P_i^{-1} M_{1.5}^{-2/3} (P_0/100ms)^{-1/3}$, which gives a kick velocity $v_k \approx 800 \chi I_{45} M_{1.5}^{-1/3} (P_0/100ms)^{-2/3} / P_i km/s$. PSR J0538 + 2817 is relatively slow with $v \approx 140 km/s$ and $P_0 \approx 130ms$, so we require an jet asymmetry $\chi \approx 0.2 P_i M_{1.5}^{1/3} / I_{45}$. Since the velocities are set at r_{in} we see that slow spin goes with slow kick in this model. Substantial jet asymmetries are required, but remain to be explained. Of course, additional mass accreted while at equilibrium reduces the required χ .

With its large P_0 and small $\theta_{\Omega-v}$, PSR J0538 + 2817 provides some of the strongest constraints on spin-kick physics. These important physics conclusions are presently based on rather limited data; clearly better images confirming the torus and refining Ψ are needed. Also, a radio interferometric proper motion can improve the velocity vector and get an independent kinematic measure of t_5 . Such data should provide a new window on neutron star core collapse and its immediate aftermath.

We thank the referee, D. Sanwal for a careful reading and useful recommendations. This work was supported by CXO grant G02-3085X.

REFERENCES

- Anderson, S.B. *et al.* 1996, ApJ, 468, L55
 Arras, P. & Lai, D. 1999, ApJ, 519, 745
 Bailes, *et al.* 1989, ApJ, 343, L53
 Cordes, J.M. & Lazio, T.J.W. 2002, ast-ph/0209161
 De Luca, A., Mignani, R.P. & Caraveo, P.A. 2000, A&A, 354, 1011
 Caraveo, P.A. & Mignani, R.P. 1999, A&A, 344, 357
 Fürst, E. & Reich, W. 1986, A&A, 163, 185
 Gotthelf, E. 2001, astro-ph/0105128
 Lai, D., Chernoff, D.F. & Cordes, J.M. 2001, ApJ, 549, 1111
 Kirschner, R. & Arnold, C.N. 1979, ApJ, 222, 147
 Mansfield, V.N. & Salpeter, E.E. 1974, ApJ, 190, 305
 Pavlov, G.G., Kargaltsev, O.Y., Sanwal, D. & Garmire, G.P. 2001, ApJ, 554, L189
 Pavlov, G.G., *et al.* 1995, in The Lives of Neutron stars, eds. M. Alpar, U. Kiziloglu & J. van Paradijs (Dordrecht: Kluwer), 71
 Pelling, R.M. *et al.* 1987, ApJ, 319, 416
 Garmire, G.P. 2001, ApJ, 554, L189
 Shull, J.M., Fesen, R.A. & Saken, J.M. 1989, ApJ, 346, 860
 Sofue, Y., Fürst, E. & Hirth, W. 1980, PASJ, 32, 1
 Spruit, H. & Phinney, E.S. 1998, Nature, 393, 139
 Sun, X. *et al.* 1996, MPE report, 263, 195
 van den Bergh, S. 1978, ApJ, 224, 1086
 Weisskopf, M.C. *et al.* 2000, ApJ, 536, L81

TABLE 1
POINT SOURCE SPECTRAL FITS

Model	kT(keV)	$N_H(10^{21}cm^{-2})$	$f_x(10^{-12}erg/cm^2/s)$	$R_{eff}(km)$	χ^2/DOF
BB	0.159±0.0017	3.1±0.2	3.3	2.6	1.03
magH	0.054±0.0007	4.7±0.2	13.7	13	0.94